Spin Rings in Semiconductor Microcavities

I. A. Shelykh,[1,2] T. C. H. Liew,[1,3] and A. V. Kavokin[3,4]
[1]*ICCMP, Universidade de Brasilia, 70904-970 Brasilia DF, Brazil*
[2]*St. Petersburg State Polytechnical University, 195251, St. Petersburg, Russia*
[3]*School of Physics and Astronomy, University of Southampton, SO17 1BJ, Southampton, United Kingdom*
[4]*Physics Faculty, University of Rome II, 1, via della Ricerca Scientifica, 00133, Roma, Italy*
(Received 28 August 2007; revised manuscript received 21 January 2008; published 18 March 2008)

New effects of self-organization and polarization pattern formation in semiconductor microcavities, operating in the nonlinear regime, are predicted and theoretically analyzed. We show that a spatially inhomogeneous elliptically polarized optical cw pump leads to the formation of a strongly circularly polarized ring in real space. This effect is due to the polarization multistability of cavity polaritons which was recently predicted. The possible switching between different stable configurations allows the realization of a localized spin memory element, suitable for an optical data storage device.

DOI: 10.1103/PhysRevLett.100.116401 PACS numbers: 71.36.+c, 42.55.Sa, 42.65.Pc

Introduction.—Self-organization and pattern formation are among the most interesting phenomena in various nonlinear systems in physics, chemistry, and biology. In quantum physics nonlinearity arises from many-particle interactions, which being treated within the framework of the mean-field approximation result in the Hartree-Fock equations for interacting fermions and the Gross-Pitaevskii (GP) equation for interacting bosons. The latter is widely used for the description of the dynamics of atomic Bose-Einstein condensates (BECs) [1]. Mathematically, the GP equation is equivalent to the nonlinear Schrödinger equation of classical nonlinear optics. It describes a variety of intriguing phenomena in nonlinear media, such as vortex formation [2], self-focusing, and soliton propagation [3].

Recently, examples of self-organization were reported in the system of interacting 2D excitons, where the formation of ring patterns in the emission distribution was experimentally observed in the nonlinear regime [4]. This phenomenon was initially attributed to the superfluid phase transition. More recent models, however, identified the crucial role of the separation of classical electron and hole plasmas with emission from the sharp circular boundary between these two regions [5]. Because of strong dephasing this phenomenon can be described by classical diffusion equations for electrons and holes, rather than by a quantum equation of the GP type for a spatially coherent excitonic BEC.

Cavity polaritons seem to be more appropriate candidates for the observation of quantum nonlinear phenomena. Being combinations of the cavity photon and 2D exciton, they have extremely small effective mass (about 10^{-4}–10^{-5} of the free electron mass) and, at the same time, they interact efficiently with one another. Polariton-polariton interactions lead to various nonlinear effects in microcavities, including parametric scattering [6] and bistability [7]. Because of the long decoherence time [8] and the fact that in the low density limit they behave as weakly interacting bosons [9], the dynamics of the polariton system can be described by the GP equation [10,11]. Being treated coherently, polariton-polariton interactions result in the suppression of Rayleigh scattering [10] and ring pattern formation [11] in polariton systems. Both effects are due to the renormalization of the dispersion of elementary excitations and an associated superfluid transition in the system.

An important peculiarity of cavity polaritons is related to their spin degree of freedom [12]. Polaritons have two possible spin projections on the structure growth axis, ± 1, corresponding to the right (σ_+) and left (σ_-) circular polarizations of emitted photons. In the case of nonzero in-plane wave vector these two components are mixed by TE-TM splitting [13]. A further mixing of the linear polarizations appears due to the spin dependent polariton-polariton interaction [14], which affects the superfluid properties of the system [11,15] and leads to remarkable nonlinear effects in polariton spin relaxation, such as self-induced Larmor precession and inversion of the linear polarization during the scattering act [12,16].

Recently, the scalar semiclassical approach based on the Gross-Pitaevskii equation was extended to account for the two polarization states of resonantly pumped cavity polaritons [17]. It was shown that the nonlinear, polarization dependent polariton-polariton interactions result in a multistability of the driven polariton mode.

In this Letter we analyze how the polarization multistability and hysteresis can lead to polarization pattern formation in realistic semiconductor microcavities.

Qualitatively, the polarization multistability and hysteresis can be understood as follows. Let us consider a quantum microcavity resonantly driven at $k = 0$ by a cw laser beam with circular polarization degree:

$$\rho_c^{\text{pump}} = \frac{P_+ - P_-}{P_+ + P_-}, \tag{1}$$

where P_+ and P_- represent the intensities of the σ_+ and σ_- components of the pump, respectively. The polariton wave function ψ_σ satisfies the driven spinor Gross-Pitaevskii equation [17], which in the stationary regime

yields a cubic equation for the dependence of the internal intensities $n_\sigma = |\psi_\sigma|^2$ on the intensities of the pump:

$$\left[\left(E_0 - E_p + n_\sigma + \frac{\alpha_2}{\alpha_1} n_{-\sigma}\right)^2 + \frac{\hbar^2}{4\tau^2}\right] n_\sigma = P_\sigma, \quad (2)$$

where $\sigma = \pm$, τ is the polariton lifetime, E_p is the cw pump energy, E_0 is the bare polariton energy, and $\alpha_{1(2)}$ is the matrix element of polariton-polariton interaction in the parallel spin (antiparallel spin) configuration, respectively. It is well known that for 2D excitons and exciton-polaritons the exchange interaction strongly dominates over the direct one, and thus polariton-polariton interactions are strongly anisotropic $|\alpha_2| \ll \alpha_1$ [18]. Equation (2) represents the behavior of only one macroscopically occupied state. The fields were rescaled so that only the ratio of α_2 to α_1 is significant. If we suppose that $\alpha_2 = 0$, then the behavior of σ_+ and σ_- polarizations becomes independent and the internal intensity of each component is given by an S-shaped curve, as shown in Fig. 1(a).

When an external pump is switched on, n_σ lies on the lower branch of its bistability curve if P_σ is less than P_1. As P_σ is increased there is a jump in n_σ at the point $P_\sigma = P_1$, corresponding to the transition to the upper branch of the bistability curve. If one then starts to decrease P_σ, the transition back to the lower branch of the bistability curve occurs at the intensity $P_\sigma = P_2$. Crucially, because the σ_+ and σ_- fields can lie on the same or different branches of the bistability curve, the system can support four stable configurations thus demonstrating multistability. There is also an associated hysteresis not only in the total intensity of the internal field but also in its circular polarization degree [17].

In order to reveal spin ring formation, let us now consider a cavity pumped by a cw Gaussian pump, with slightly positive circular polarization degree, oriented at normal incidence. The dynamics of the system is described by the driven spinor GP equation:

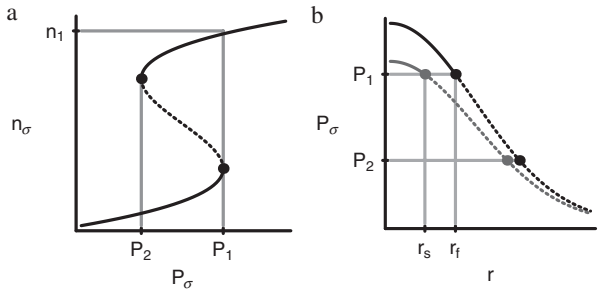

FIG. 1. (a) The spinor polariton population n_σ as a function of pumping intensity P_σ for a single polariton state. With increasing intensity, the population n_σ jumps when $P_\sigma = P_1$ to the upper branch of the bistability curve. (b) Gaussian pump profile showing the σ_+ polarized intensity (black) and σ_- intensity (gray). When P_σ is greater than P_1 (solid part of curves), n_σ lies on the upper branch of its bistability curve, otherwise (dashed part) it lies on the lower branch.

$$i\hbar \frac{\partial \psi_\sigma}{\partial t} = \left(\hat{E}_{\mathrm{LP}}(-i\hat{\nabla}) - \frac{i\hbar}{2\tau}\right)\psi_\sigma + \left(|\psi_\sigma|^2 + \frac{\alpha_2}{\alpha_1}|\psi_{-\sigma}|^2\right)\psi_\sigma + p_\sigma(\mathbf{r}, t)e^{-iE_p t/\hbar}, \quad (3)$$

where the σ polarized internal cavity polariton field ψ_σ depends on the spatial coordinate $\mathbf{r}$. The kinetic energy operator $\hat{E}_{\mathrm{LP}}$ represents the dispersion of the lower polariton branch (the operator depends on the Laplacian operator). The pump field is given by $p_\sigma(\mathbf{r}, t) = A_\sigma e^{-\mathbf{r}^2/R^2}$, where A_σ are the peak amplitudes.

To understand the situation qualitatively we first consider the case $\alpha_2 = 0$, $0 < \rho_c^{\mathrm{pump}} \ll 1$, and neglect the kinetic energy term; that is, we assume an infinite polariton effective mass. In this limit the spreading of particles in real space is suppressed and the polarization dynamics at a given point in space depends only on the pump intensity at that point. This allows a simple analytical consideration of the polarization distribution in real space using Eq. (2). The intensity profile, $P_\sigma(r) = |p_\sigma(r)|^2$, of the pump is illustrated in Fig. 1(b), where the black and gray curves show $P_+(r)$ and $P_-(r)$, respectively. Close to $r = 0$ the intensity of the pump is large enough such that both n_+ and n_- lie on the upper branch of their bistability curves. In this case the circular polarization degree would be small. However, beyond

$$r_s = R\sqrt{\frac{1}{2}\ln\left(\frac{A_-^2}{P_1}\right)}, \quad (4)$$

the intensity of P_- is too small for n_- to be on the upper branch. Hence we expect a region of strong circular polarization, since n_+ remains on the upper branch. This region continues until the point

$$r_f = R\sqrt{\frac{1}{2}\ln\left(\frac{A_+^2}{P_1}\right)}, \quad (5)$$

beyond which P_+ is also too small for n_+ to be on the upper branch and we again have a low circular polarization degree. In other words we expect a strongly circularly polarized ring (spin ring) to appear in the spatial emission pattern, starting from $r = r_s$ and finishing at $r = r_f$.

Numerical results.—The finite effective mass of polaritons should lead to the spreading of the polarized ring in real space. To accurately account for this effect we return to Eq. (4) and solve numerically using a time propagation method. To minimize the number of parameters in our model we consider a parabolic dispersion (this is still realistic since we consider excitation at $k = 0$) described by an effective mass m. Our results are shown in Fig. 2.

We clearly see that a ring of circular polarization appears in real space [2(b)] and there are associated steplike changes in the total intensity [2(a)] caused by changes of n_σ between upper and lower branches. However, we notice that the size of the ring has expanded after the initial switch on of the pump [Figs. 2(c) and 2(d)]. When one examines

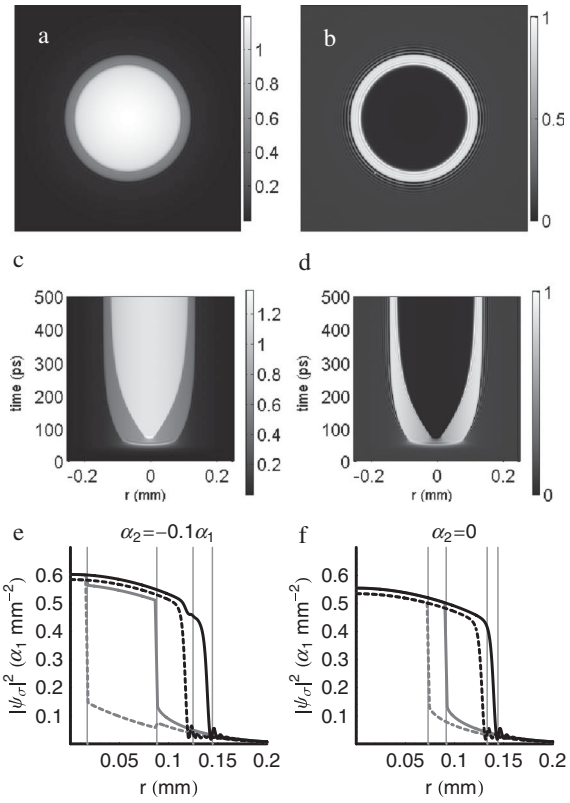

FIG. 2. Polariton field caused by excitation with a Gaussian pump with $\rho_c^{\text{pump}} = 0.1$. (a) The total intensity of the polariton field in a 0.25×0.25 mm area in real space at $t = 500$ ps (when quasiequilibrium is established). (b) The corresponding circular polarization degree. (c) The time dependence of the total intensity of a radial slice in real space. (d) Time dependence of the circular polarization degree. Parameters used for (a)–(d): $\tau = 3$ ps, $\alpha_2/\alpha_1 = -0.1$, $E_p - E_{\text{LP}}(0) = 0.4$ meV, $R = 0.17$ mm, $m = 10^{-4} \times m_e$ (m_e is the free electron mass). The pump is switched on at $t = 50$ ps. (e) Cross section of the fields (at $t = 500$ ps) showing n_+ (solid line) and n_- (dashed line) for the case of finite (black) and infinite effective mass (gray). Vertical lines show the radii at which turning points in the S-shaped curves [shown by spots in Fig. 1(b)] occur. These can be calculated from Eq. (2) or by using a diagram like Fig. 3 of Ref. [17]. (f) The same as (e) but for the case $\alpha_2 = 0$.

the profile of the ring [Fig. 2(e)] after some time one finds that the ring appears with greater radii than that predicted by Eqs. (4) and (5). This is also the case when $\alpha_2 = 0$ [see Fig. 2(f)], although we see that in the case of infinite polariton effective mass the ring does form where we expect from Eqs. (4) and (5).

The increase in the ring radii is due to the propagation of polaritons in real space, which tends to smooth the density distribution. Although the ring may initially form as we expect with external radius r_f, the propagation of polaritons means that the region immediately beyond r_f also switches to the upper branch (for the σ_+ component). Once this region has switched, the further propagation of polaritons allows the next region to switch and so the ring expands. However, the ring cannot continue to expand forever since eventually we reach the point where $P_+ = P_2$. Beyond this point there is no upper branch for the n_+ field to switch to. Exactly the same account holds true for the σ_- polarization and the end result is that the ring radii are increased. This increase does not depend on the effective mass of polaritons; changing the effective mass only changes the time required for polaritons to obtain the larger radii (for infinite effective mass the time is infinite). The larger radii are given by similar equations to Eqs. (4) and (5) with the difference that P_1 is replaced by P_2. Figure 2(f) shows that for $\alpha_2 = 0$ the ring appears with radii given by $P_\sigma = P_2$ in the case of finite effective mass.

We note that no elastic parametric scattering was observed in our calculations. Although such scattering is automatically accounted for by the Gross-Pitaevskii equations, our parameters are parametrically stable, which can be checked using the methods used in Ref. [19]. We also note that the transverse effects studied in the present Letter are unrelated to the use of a wedge-shaped sample and thus are different from those studied experimentally in Ref. [20].

Polarization control of localized states.—For practical applications, such as optical data storage, it is useful to be able to switch between the stable states in a system [21]. We now consider an experiment that can achieve such switching using various pulses. We will create a localized polariton state using a cw linearly polarized Gaussian beam with intensities $P_2 < P_\sigma < P_1$. In this case both n_+ and n_- lie on the lower branch of the bistability curve after the pump is switched on (at $t = 50$ ps in our calculation). We then consider excitation with successive pulses of σ_+ and σ_- polarizations. These pulses are chosen to be in phase with the cw pump. They are able to independently switch n_+ and n_- to the upper branch of the bistability curve. We can then apply pulses of σ_+ and σ_- polarizations, which are out of phase with the cw pump. The application of a pulse P_σ that is out of phase causes the n_σ

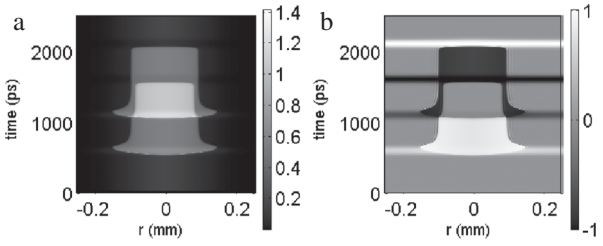

FIG. 3. Temporal dynamics of the total polariton intensity (a) and circular polarization degree (b) in real space for a polarization switching experiment. A linearly polarized Gaussian pump is turned on at $t = 50$ ps. Pulses arrive at 550, 1050, 1550, and 2050 ps, with σ_+, σ_-, σ_+, and σ_- polarizations, respectively. The first two pulses are in phase with the cw pump; the second two are out of phase. The other parameters were identical to those used in Fig. 2.

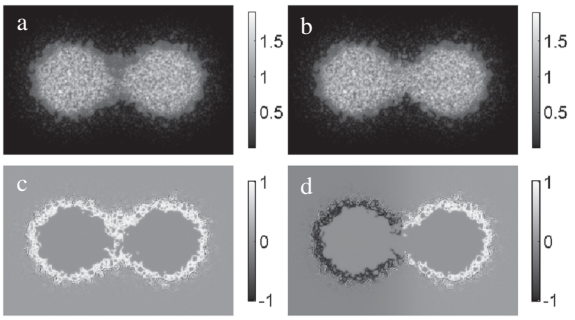

FIG. 4. Intensity of overlapping identically (a) and oppositely polarized spin rings (b) in a 0.4×0.2 mm region in space. (c),(d) show the corresponding circular polarization degrees. The parameters used were the same as in Fig. 2 but including a disorder potential with a Gaussian correlation length of 2 μm and a root mean squared value of 0.2 meV.

component to return to the lower branch. The full sequence of results is shown in Fig. 3.

In this way we can achieve full control of the polarization of a localized state using various switching pulses. In our calculations the response time is less that 10 ps. The threshold power to observe such an effect should be much smaller than that required in conventional nonlinear optical systems [22]; due to the strength of the polariton interactions, the threshold power for observing bistability is estimated to be 4 orders of magnitude lower [17].

Disorder and interaction between spin rings.—In realistic microcavities, polaritons are subject to a static disorder potential arising from cavity width variations. To check the effect of disorder on polarization patterns we introduced a disorder potential [23] into Eq. (3). We considered two overlapping spin rings (Fig. 4) excited by elliptically polarized Gaussian beams with either identical or opposite circular polarization degrees. Our results show that although the disorder distorts spin rings, they can still be observed in an experiment. The midway point between the spin rings is strongly circularly polarized if the rings are copolarized, yet it is linearly polarized if the rings have opposite circular polarization degrees.

Conclusions.—We have demonstrated theoretically how rings of strong circular polarization (spin rings) can be realized in semiconductor microcavities by using a spatially inhomogenous cw laser excitation. The radii of these rings was estimated analytically. The experimental observation of the rings would demonstrate the existence of polarization multistability in semiconductor microcavities. Using various pulses, the polarization multistability, allows one to switch the polarization of a localized polariton state. Such control could form the basis for an optical data storage device.

We thank F. P. Laussy and G. Malpuech for useful discussions. I. A. S. acknowledges support from the Grant of the President of Russian Federation. T. C. H. L. acknowledges support from the EPSRC.

[1] F. Dalfovo *et al.*, Rev. Mod. Phys. **71**, 463 (1999); A. J. Legett, Rev. Mod. Phys. **73**, 307 (2001); L. Pitaevskii and S. Stringari, *Bose-Einstein Condensation* (Oxford University, New York, 2003).
[2] M. J. Quist, Phys. Rev. B **60**, 4240 (1999).
[3] Yu. S. Kivshar and G. Agrawal, *Optical Solitons: From Fibers to Photonic Crystals* (Academic, New York, 2003).
[4] L. V. Butov, A. C. Gossard, and D. S. Chemla, Nature (London) **418**, 751 (2002); D. Snoke *et al.*, Nature (London) **418**, 754 (2002).
[5] R. Rapaport *et al.*, Phys. Rev. Lett. **92**, 117405 (2004); L. V. Butov *et al.*, Phys. Rev. Lett. **92**, 117404 (2004); A. L. Ivanov *et al.*, Europhys. Lett. **73**, 920 (2006).
[6] P. G. Savvidis *et al.*, Phys. Rev. Lett. **84**, 1547 (2000); A. I. Tartakovski *et al.*, Phys. Rev. B **62**, R13 298 (2000); R. M. Stevenson *et al.*, Phys. Rev. Lett. **85**, 3680 (2000); C. Ciuti *et al.*, Phys. Rev. B **63**, 041303 (2001).
[7] A. Baas *et al.*, Phys. Rev. B **70**, 161307(R) (2004); N. A. Gippius *et al.*, Europhys. Lett. **67**, 997 (2004); D. M. Whittaker, Phys. Rev. B **71**, 115301 (2005).
[8] W. Langbein *et al.*, Phys. Rev. B **75**, 075323 (2007).
[9] Polariton BEC was observed recently; see J. Kasprzak *et al.*, Nature (London) **443**, 409 (2006).
[10] I. Carusotto and C. Ciuti, Phys. Rev. Lett. **93**, 166401 (2004).
[11] I. A. Shelykh *et al.*, Phys. Rev. Lett. **97**, 066402 (2006).
[12] For a review on spin properties of cavity polaritons, see I. A. Shelykh *et al.*, Phys. Status Solidi B **242**, 2271 (2005).
[13] G. Panzarini *et al.*, Phys. Rev. B **59**, 5082 (1999).
[14] F. P. Laussy *et al.*, Phys. Rev. B **73**, 035315 (2006).
[15] Yu. G. Rubo *et al.*, Phys. Lett. A **358**, 227 (2006); I. A. Shelykh *et al.*, Superlattices Microstruct. **41**, 313 (2007).
[16] D. N. Krizhanovskii *et al.*, Phys. Rev. B **73**, 073303 (2006).
[17] N. A. Gippius *et al.*, Phys. Rev. Lett. **98**, 236401 (2007).
[18] C. Ciuti *et al.*, Phys. Rev. B **58**, 7926 (1998); M. Combescot and O. Betbeder-Matibet, Phys. Rev. B **74**, 125316 (2006); P. Renucci *et al.*, Phys. Rev. B **72**, 075317 (2005).
[19] M. Wouters and I. Carusotto, Phys. Rev. B **75**, 075332 (2007).
[20] A. Baas, J. Ph. Karr, H. Eleuch, and E. Giacobino, Phys. Rev. A **69**, 023809 (2004).
[21] H. M. Gibbs *Optical Bistability: Controlling Light with Light* (Academic, New York, 1985).
[22] G. S. McDonald and W. J. Firth, J. Opt. Soc. Am. B **10**, 1081 (1993); M. Brambilla, L. A. Lugiato, and M. Stefani, Europhys. Lett. **34**, 109 (1996).
[23] V. Savona and W. Langbein, Phys. Rev. B **74**, 075311 (2006).